Integrative discovery of a multimodal cancer immunotherapy using machine learning and viral vector engineering

Qiuchen Guo[1], Shane Kammerman[1], John D. Christie[1], Matthew Wai Heng Chung[2], William Guesdon[2], Elton Yechao Zhu[3], David Krisky[1], Karen Bouch[1], Paul P. Tak[1], Francesca Barone[1], Anne R. Diers[1]
[1]Candel Therapeutics, Needham, MA, USA, [2]Sonrai, Belfast, Northern Ireland, [3]Independent Researcher, Boston, MA, USA

Abstract# 893

Presented at SITC's 40th Anniversary Annual Meeting, November 2025

The enLIGHTEN™ Discovery Platform

- A major challenge in overcoming the immunosuppressive tumor microenvironment (TME) and tumor heterogeneity is the rational identification of TME-associated targets whose simultaneous modulation can reverse immune suppression and enhance therapeutic efficacy.
- Critically, the optimal combination of immune targets varies across tumor types, reflecting distinct TME landscapes.
- To address this challenge, we developed enLIGHTEN™, a discovery platform that integrates machine learning, viral vector engineering, and rapid payload validation to design programmable viral immunotherapies tailored to modulate multiple immune pathways within the TME with the goal of overcoming resistance and improving responses.

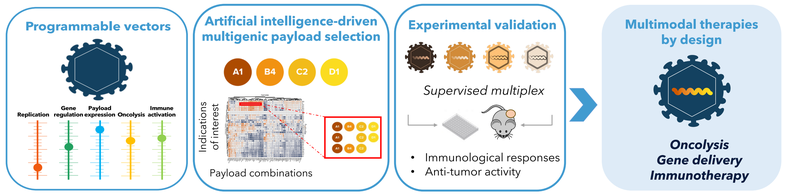

Alpha-201: a programmable vector for immune activation

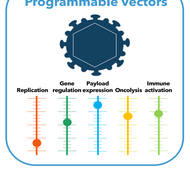

Alpha-201, a replication-defective vector, was selected as the programmable vector for its properties of **enhanced immuno-stimulation** (Fig. 1, 2), **regulated oncolysis** (Fig. 3) and **sustained payload expression** (Fig. 4).

Enhanced immuno-stimulation

Figure 1

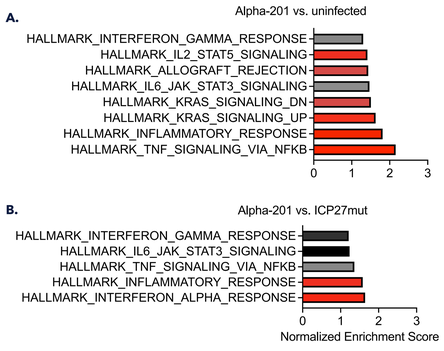

Figure 1: Gene Set Enrichment Analysis (GSEA) was performed on RNAseq data, and top pathways enriched in cells infected with Alpha-201 compared with uninfected (**A**) or ICP27mut vector (**B**).

Figure 2

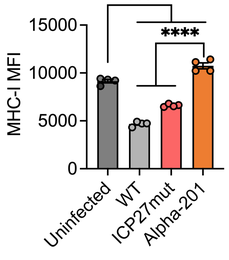

Figure 2: Hs578T cells were infected with 10 PFU/cell Alpha-201 or ICP27mut vector. Cell-surface expression of MHC class was assessed by flow cytometry 24h after infection. N=4. ANOVA with Tukey's correction. ***p<0.001, ****p<0.0001.

Regulated oncolysis

Figure 3

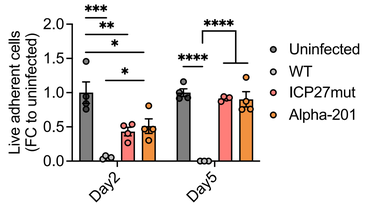

Sustained payload expression

Figure 4

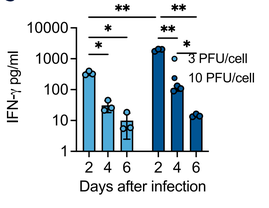

Figure 3: Hs578T cells were infected with 10 PFU/cell of indicated vector. Number of live adherent cells were quantified 2 or 5 days after infection. N=4. ANOVA with Tukey's correction. *p<0.05, **p<0.01, ***p<0.001, ****p<0.0001.

Figure 4: IFN-γ production rate from Hs578T cells infected with Alpha-201-IFN-γ and conditioned medium analyzed by ELISA. N=3. ANOVA with Tukey's correction. *p<0.05, **p<0.01.

Artificial intelligence-driven multigenic payload selection

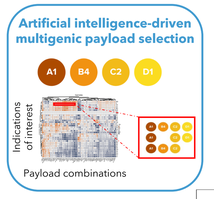

In order to select the optimal payload combination to encode in the Alpha-201 vector, we applied the enLIGHTEN™ platform to publicly available datasets to identify indication-specific, TME properties associated with clinical outcome. The algorithm provided higher scores to single genes more strongly associated with improved survival through TME effects (Fig. 5). **IFN-γ, IL-12, IL-15, and IL-21** were selected for experimental validation.

Figure 5

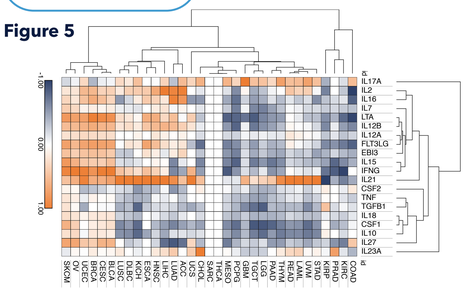

Figure 5: Heatmap showing the contribution scores of each payload gene to survival outcomes across TCGA cancer types. Scores were calculated by integrating CoxPH coefficients (TME properties to survival) and linear regression coefficients (gene to TME properties), reflecting the combined effect of gene expression on immune cell composition and survival. Positive scores (orange) indicate improved survival, while negative scores (blue) indicate worse survival.

Ex vivo multiplex evaluation enables rational payload prioritization

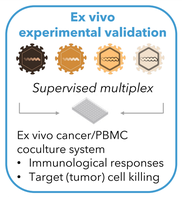

Infection of cancer cells with in silico selected payload combinations using single gene encoding Alpha-201 vectors induced PBMC-mediated cancer cell killing in an infection- and payload-dependent manner (Fig. 6). Target cell killing was associated with significant changes in the composition and function of immune cells within the coculture (Fig. 7, 8). The combination of IL-12 and IL-15 was then prioritized for in vivo testing based on its effects on multiple parameters.

Figure 6

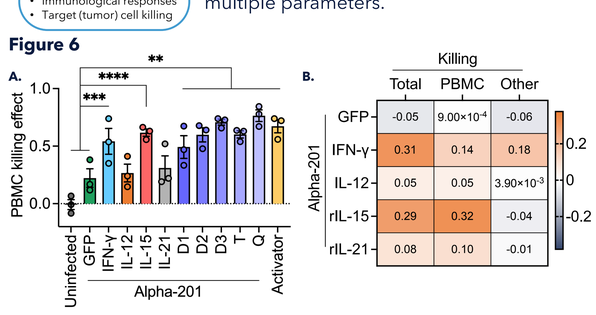

Figure 6: Hs578T cells were infected with Alpha-201 encoding GFP, IFN-γ, or other vectors individually or in multiplexes (total vector: 1 PFU/cell), then cultured ± PBMC for 72 h. D1: IFN-γ, IL-12; D2: IFN-γ, IL-15; D3: IL-12, IL-15; T: IFN-γ, IL-12, IL-15; Q: IFN-γ, IL-12, IL-15, IL-21 **A.** PBMC-mediated target cell killing was assessed by flow cytometry. **B.** Association of target cell killing with each payload was analyzed by OLS regression.

Figure 7

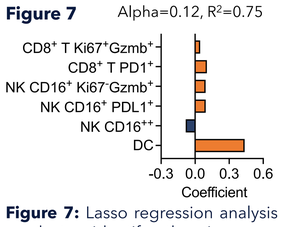

Figure 7: Lasso regression analysis was used to identify the immune cell populations positively (orange bars) or negatively (blue bar) correlated with PBMC-mediated tumor cell killing.

Figure 8

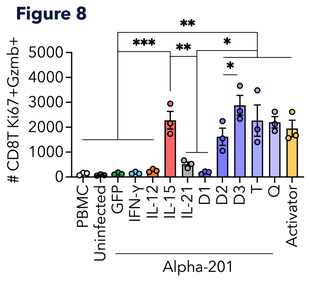

Figure 8: Total cell number by supervised multiplex condition for the immune populations associated with the PBMC-mediated tumor cell killing. N=3. ANOVA with Tukey's correction. *p<0.05, **p<0.01, ***p<0.001.

Figure 9

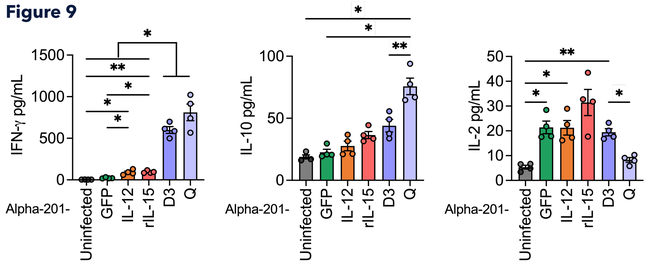

Figure 9: Conditioned medium was collected after 3 days of PBMC-tumor cell coculture and IFN-γ, IL-10 and IL-2 levels were measured. N=4. *p<0.05, **p<0.01.

Contact:
info@candeltx.com

Robust in vivo anti-tumor efficacy upon delivery of IL-12 and IL-15

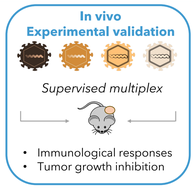

Intratumoral treatment with Alpha-201 vectors encoding IL-12 and IL-15 resulted in significant tumor growth inhibition (Fig. 10). Increases in multiple immune cell types within tumors (Fig. 11) and immune activation, both within tumors (Fig. 12) and in the periphery (Fig. 13), were observed and associated with this antitumor activity.

Figure 10

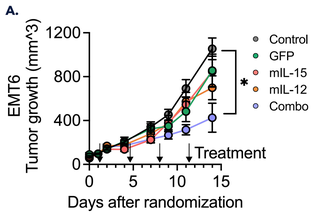

B.

Alpha-201-			
mIL-12 (E_{IL12})	mIL-15 (E_{IL15})	Combo (E_C)	Synergy effect $T=(1-E_{IL12})\times(1-E_{IL15})-(1-E_C)$
20%	-4.8%	62.4%	46% (P=0.0086)

Figure 10: A. Growth kinetics of EMT6 tumors treated with Alpha-201 vectors (3E7 PFU/dose). N=8 mice per group. *p<0.05. **B.** Payload synergy calculation for tumor growth inhibition (TGI) rate for each treatment condition relative to Alpha-201-GFP from Panel A.

Figure 11

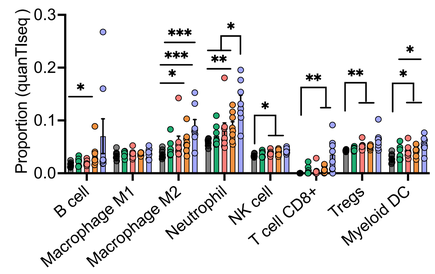

Figure 11: Bulk RNAseq was performed on tumors harvested at Day 14, and immune cell composition deconvoluted from the bulk RNAseq data. N=8 mice per group. *p<0.05, **p<0.01, ***p<0.001.

Figure 12

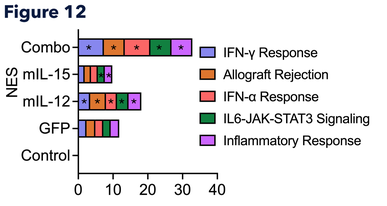

Figure 13

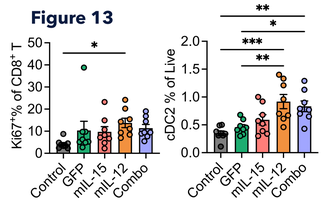

Figure 12: Hallmark pathways analysis (GSEA) was performed on bulk RNAseq data from EMT6 tumors collected on Day 14, and the normalized enrichment scores (NES) are shown. *p<0.05.
Figure 13: Flow cytometry analysis of PBMC from tumor bearing mice. N=8 mice per group. *p<0.05, **p<0.01, ***p<0.001.

Consistent immune response to viral payload delivery ex vivo and in vivo

Comparative analysis of immune responses across different models revealed that alterations in PBMC populations from ex vivo cocultures closely mirrored those observed in tumor-bearing animals treated with Alpha-201-mIL-12 and IL-15 (Fig. 14).

Figure 14

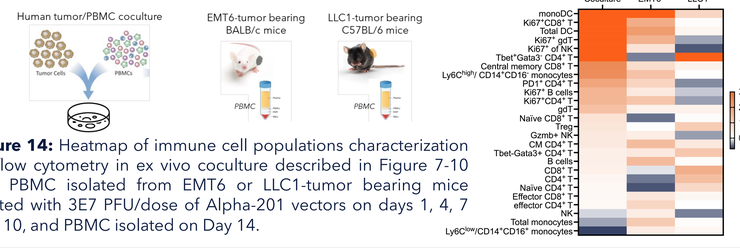

Figure 14: Heatmap of immune cell populations characterization by flow cytometry in ex vivo coculture described in Figure 7-10 and PBMC isolated from EMT6 or LLC1-tumor bearing mice treated with 3E7 PFU/dose of Alpha-201 vectors on days 1, 4, 7 and 10, and PBMC isolated on Day 14.

Conclusions

- enLIGHTEN™ enables the rational design of multimodal viral immunotherapies by integrating computational predictions with experimental validation.
- Alpha-201-IL-12 and IL-15 showed strong immune activation and tumor suppression in breast cancer, demonstrating potential of enLIGHTEN™ to guide indication-specific immunotherapy development.